FILE COPY
NO. 1-W

NATIONAL ADVISORY COMMITTEE FOR AERONAUTICS

WARTIME REPORT

ORIGINALLY ISSUED
October 1943 as
Advance Restricted Report 3J27

CRITICAL STRESSES FOR PLATES

By Eugene E. Lundquist and Evan H. Schuette

Langley Memorial Aeronautical Laboratory
Langley Field, Va.

FILE COPY
To be returned to
the files of the National
Advisory Committee
for Aeronautics
Washington D. C.

NACA

WASHINGTON

NACA WARTIME REPORTS are reprints of papers originally issued to provide rapid distribution of advance research results to an authorized group requiring them for the war effort. They were previously held under a security status but are now unclassified. Some of these reports were not technically edited. All have been reproduced without change in order to expedite general distribution.

NATIONAL ADVISORY COMMITTEE FOR AERONAUTICS

ADVANCE RESTRICTED REPORT

L-466

CRITICAL STRESSES FOR PLATES

By Eugene E. Lundquist and Evan H. Schuette

SUMMARY

The paper is a review of a part of the work done by the National Advisory Committee for Aeronautics on the critical stresses for plates in compression and in shear, as well as in combined direct stress and shear.

The theoretical work of calculating the critical stress for plates with elastically restrained edges is subdivided into a series of basic problems for which design charts and curves are prepared. The principles of the Cross method of moment distribution are used to provide a new approach to the solution of problems in the stability of structures composed of plates.

The basic methods of the theoretical approach are outlined, but the main emphasis is on the practical significance and use of the results of both theoretical studies and laboratory tests concerned with the buckling of plates.

INTRODUCTION

If a structure composed of plates is so loaded that the plate elements are subjected to compression, shear, or combined direct stress and shear, the maximum strength of the structure may be determined by the critical stress (the stress at which buckling occurs). Even when the maximum strength is greater than the critical value, the strength of the structure is related to the critical stress. It is therefore important in many structural calculations to be able to predict the critical stress for plates if the structural elements are to be efficiently designed. These considerations, in addition to the need for accurately maintaining the contour of wing

surfaces in flight, make it desirable to have, for ready use in design, methods for calculating the critical stress for plates.

The classical methods of calculating critical stresses for plates have not always been carried to the point where the results can be easily applied to many of the complex problems encountered in design. For a number of years, the structures research section of the National Advisory Committee for Aeronautics has studied this problem for the purpose of breaking it down into its basic elements in order that practical solutions of more difficult problems might be made from the solution for the basic cases with no more than a few arithmetical computations. Tests have also been made to verify a part of the theoretical work. Some of the theoretical methods and experimental results have been summarized in the present paper, with emphasis on the more practical aspects of the problem.

The paper was originally presented before the A. S. M. E. joint meeting of the aviation and applied mechanics division at Los Angeles, Calif. on June 15, 1943.

PRINCIPLES OF MOMENT DISTRIBUTION APPLIED TO STABILITY OF FLAT-PLATE STRUCTURES IN COMPRESSION

The principles of moment distribution were shown in reference 1 to be applicable to the study of the stability of structures composed of bars under axial load. The fundamental character of the quantities used in the method of moment distribution and the formulas associated with them make possible, by suitable definition of "stiffness" and "carry-over factor," the application of an analysis like that of reference 1 to a study of the stability of structures composed of plates under compressive load. Before these definitions are given, a description of the manner in which the moments are distributed along the edges of the plate is desirable.

The solution of the differential equation for the critical compressive stress of an infinitely long plate with given edge restraints reveals that, when the plate buckles, the moments and the rotations at both edges of the plate vary sinusoidally along the edges and are in phase with each other. The ratio of moment per unit length at any point along the edge to the rotation at

that point is therefore constant along the edge for a given wave length. From these considerations, it is possible to write the following definitions of stiffness and carry-over factor:

Stiffness.- If an infinitely long flat plate is under longitudinal compression with one unloaded edge on an unyielding support, the ratio of moment per unit length at any point along this unloaded edge to the rotation in quarter-radians at that point when the moment is distributed sinusoidally is called the stiffness of the plate.

Carry-over factor.- The ratio of the moment per unit length developed at any point along the far unloaded edge to the applied moment per unit length at the corresponding position along the near unloaded edge is called the carry-over factor of the plate.

The symbols used to designate the stiffness and the carry-over factor for the different types of support and restraint at the far edge are given in the following table:

Stiffness	Carry-over factor	Conditions at far edge
S	C	Far edge supported and fixed against rotation
S^{I}	C^{I}	Far edge supported and elastically restrained against rotation
S^{II}	$C^{II} = 0$	Far edge supported with no restraint against rotation
S^{III}	$C^{III} = 0$	Far edge free (no support and no restraint against rotation)
S^{IV}	$C^{IV} = -1$	Far edge supported and subjected to moment equal and opposite to that applied at near edge

Figures 1 to 3 show the direction of compressive load and examples of the sinusoidally distributed moments along the unloaded edges of the plate.

In a structure composed of plates, it is assumed that the joints between plates, or between plates and longitudinal restraining members, remain in their original straight lines but are free to rotate subject to the elastic restraint of the interconnecting plates and members. If a sinusoidally distributed external moment is applied along an edge common to more than one plate (fig. 4), it follows, from a moment-distribution analysis similar to that made in reference 1 for the case of bars, that the plates will be stable if

$$\Sigma S^{I}_{ij} > 0 \qquad (1)$$

The condition of neutral stability gives the critical buckling load for the assembly of plates and is obtained by setting the stiffness stability factor equal to zero, or

$$\Sigma S^{I}_{ij} = 0 \qquad (2)$$

If the assembly is symmetrical about an edge of one plate, the fewest computations would be involved if equation (2) were applied at that edge. In the case of an assembly of plates symmetrical about one plate, it is advantageous to apply equal and opposite moments at the two edges of the plate about which the assembly is symmetrical. (See fig. 5.) For this case, equation (2) can be written as follows:

$$S^{IV}_{ij} + \Sigma S^{I}_{ih} = 0 \qquad (3)$$

The use of equation (3) instead of equation (2) is recommended when the assembly of plates is symmetrical about a plate.

The methods of moment distribution as applied to the stability of plates are more completely presented in reference 2, where an illustrative problem is solved in detail. Reference 3 presents tables of stiffness and carry-over factor required in the solution of practical problems.

INSTABILITY OF THE WEB AND FLANGES OF CHANNEL- AND Z-SECTION COLUMNS

The methods of moment distribution, together with variations of these methods employing the charts of references 4 and 5, have been used to calculate the critical compressive stress for plate buckling of a family of I-, Z-, channel, and rectangular-tube sections (reference 6). Figure 6 presents the results of this work as applied to channel- and Z-section columns, where k_W is the coefficient in the equation

$$\frac{\sigma_{cr}}{\eta} = \frac{k_W \pi^2 E t_W^2}{12(1-\mu^2) b_W^2} \qquad (4)$$

The symbols in equation (4) and figure 6 are defined as follows:

σ_{cr}	critical compressive stress
k_W	nondimensional coefficient dependent upon relative dimensions of cross section
t_F, b_F, t_W, b_W	dimensions of cross section, shown in figure 6
E	modulus of elasticity
μ	Poisson's ratio
η	nondimensional coefficient that takes into account reduction of modulus of elasticity for stresses above the elastic range. Within the elastic range, $\eta = 1$

For use of equation (4) when the stresses are above the elastic range, σ_{cr}/η is evaluated first and σ_{cr} is determined from an experimentally estimated relationship between σ_{cr}/η and σ_{cr}, which is subsequently presented in this paper.

All the quantities on the right-hand side of equation (4) are known except the coefficient k_W. This value may be read from the chart of figure 6 after the necessary dimension ratios are computed and applies

whenever the length of the column is greater than several (3 or 4) times the width of the widest plate element.

In general, when a column of Z- or channel section fails by local instability, one of the two elements (web and flange) of the cross section may be said to be primarily responsible for the instability; that is, as the load approaches its critical value, this one element is no longer capable in itself of supporting the loads that are imposed on it without buckling and is requiring a certain amount of restraint from the other element of the cross section in order to delay buckling until the load is reached for which the cross section as a whole becomes unstable. The chart of figure 6 shows which element is being restrained from buckling by the other element of the cross section. A dashed line is drawn on the chart connecting the points for which the two elements are equally responsible for the instability of the section. This line divides the chart into two regions; in one region the web is primarily responsible for instability and in the other the flange is primarily responsible for instability. A column with a given cross section will fall in one of these two regions, depending on the values of the various dimension ratios. The significance of the shaded area in figure 6 will be discussed in the following section.

DIMENSIONS OF CHANNEL- OR Z-SECTION COLUMNS FOR MAXIMUM CRITICAL STRESS

The critical stress for the Z or channel column in terms of the width and thickness of the web is given by equation (4). The effect of the presence of flanges was accounted for in the evaluation of the coefficient k_w. For the purpose of studying the dimensions that give maximum critical stress, the form of equation (4) should be preserved but the concept of certain terms should be generalized.

The ratio b/t of a plate may be called the aspect ratio of the cross section of the plate. A corresponding quantity, which expresses the section aspect ratio for a thin-metal column, is the area of the section divided by the square of some thickness. If, therefore, equation (4) is written

$$\frac{\sigma_{cr}}{\eta} = k_{sec} \frac{\pi^2 E}{12(1-\mu^2)} \left(\frac{t_w^2}{A}\right)^2 \qquad (5)$$

the value of k_{sec} is a measure of the effect of the shape of the section b_F/b_W on σ_{cr}/η for a given section aspect ratio as defined by A/t_W^2 and for a given value of t_W/t_F. In figure 7 these values of k_{sec} are plotted for channel- and Z-section columns.

As a practical problem in the determination of the dimensions of a channel- or a Z-section column for the development of maximum critical stress, consider a flat strip of metal of constant thickness that is to be formed into a Z or channel. In the formed section, $t_W/t_F = 1$. The section aspect ratio A/t_W^2 is equal to the width of this strip (or the developed length of the final cross section) divided by the thickness. When bent to form a channel- or Z-section column, this strip of metal of constant thickness develops the highest σ_{cr}/η for instability of the flanges and webs if the bends are so located that the ratio of flange width to web width b_F/b_W is about 0.41, which gives the maximum value on the curve for $t_W/t_F = 1$ in figure 7.

Regardless of the thickness used in the definition of the section aspect ratio, the maximum value of σ_{cr}/η for a given value of the section aspect ratio will occur at the same values of b_F/b_W for a particular value of the ratio t_W/t_F. The maximum for each t_W/t_F ratio therefore reveals the value of b_F/b_W that the channel or Z-section should have if maximum σ_{cr}/η is desired.

Equation (4) and figure 6 are probably more useful to practical designers than the more general equation (5) and figure 7. The region covered by the near-maximum values of the curves of figure 7 is therefore indicated as a shaded area in figure 6. It is of interest to observe that the shaded area does not always enclose the dashed line that shows the dimension ratios for which the web and the flange are equally responsible for the instability of the section.

The foregoing discussion of the shapes required for maximum σ_{cr}/η is presented in more detail in

reference 6, which also presents similar material as applied to other types of cross section.

COMPRESSION TESTS OF CHANNEL, Z-, AND H-SECTIONS FOR STUDY OF INSTABILITY OF THE WEB AND FLANGES

In order to check the practical accuracy of the chart of figure 6, as well as of similar charts for other types of cross section, and also to establish experimentally the relationship between σ_{cr} and σ_{cr}/η, compression tests are being made on channel, Z-, and H-sections of 24S-T aluminum alloy as described in detail in reference 7. Figure 8 shows a test specimen after buckling. The critical loads were determined by means of wire-resistance strain gages, as well as by means of extension arms attached to the free edges of the flanges. The optical micrometer in figure 8 was used to measure the relative deflection of the extension arms.

Figure 9 shows a typical set of test data. The difference in strain on opposite sides of the specimen, as measured by the strain gages, was regarded as a measure of the curvature of the buckled web or flange. The relative movement of the extension arms was regarded as a measure of the over-all distortion of the cross section. Figure 9 shows that the curvature and distortion readings, when plotted to suitable scales, gave essentially identical curves. The critical stress was taken at about the top of the knee on these curves. This critical stress always occurred near the point where the strain gage on one side of the web or flange began to show a reduction in strain with further increase in load. (Compare curves of fig. 9(b) and (c) with curve of fig. 9(a).)

The value of σ_{cr}/η was computed for all test specimens by use of equation (4) and figure 6, or from similar equations and charts for other types of cross section. The experimental value of σ_{cr} was then plotted against this computed value of σ_{cr}/η in figure 10. The fact that σ_{cr} and σ_{cr}/η agree in the lower stress range, where $\eta = 1$, proves the accuracy of the theoretical methods. The fact that the test points establish essentially a single curve throughout the entire stress range indicates that a single effective modulus ηE can

be used for all the types of cross section studied. If it is desired actually to evaluate this modulus, the value of η can be determined from the ratio of values of σ_{cr} and σ_{cr}/η taken from this curve.

As the maximum strength developed after buckling is related to the critical stress, the experimental values of σ_{cr} were plotted against the ratio σ_{cr}/σ_{max} in figure 11. This figure shows that for the Z-section columns, the critical stress tends to be about 4 percent less than the maximum stress for critical stresses above about 32,000 pounds per square inch. The same condition exists for the channel-section columns for critical stresses above about 36,000 pounds per square inch. Below 36,000 pounds per square inch, the data for channel- and Z-section columns plot along separate curves. As the experimental investigation of which these data are a part is still in progress, no attempt will be made here to explain the difference. The discussion that follows applies to only the Z-sections, for which more extensive data are at present available.

The curve of figure 11 defines a relationship between σ_{cr} and σ_{max}. The value of σ_{cr} can be determined for a Z-section column by use of the theoretical methods previously outlined and the curve of figure 10. The value of σ_{max} is therefore also defined for a given Z-section column. The variation of σ_{max} with σ_{cr}/η is presented in figure 12. The points are experimental values of σ_{max} plotted against the computed values of σ_{cr}/η, and the curve is established by the two curves previously drawn in figures 10 and 11.

DESIGN CHARTS FOR Z-SECTION COLUMNS THAT DEVELOP INSTABILITY OF WEB AND FLANGE

The theory and experimental data of the foregoing sections provide the basic information required for the construction of practical design charts. Figures 13 and 14 are such charts prepared for Z-section columns with web and flange of equal thickness ($t_W/t_F = 1$).

These charts are useful for either extruded sections of 24S-T or sections formed from flat 24S-T sheet. No corrections have been made for reduction to minimum guaranteed properties; the charts therefore apply to 24S-T material of average properties as supplied by the Aluminum Company of America.

CRITICAL STRESS FOR FLAT PLATES UNDER COMBINED SHEAR AND DIRECT STRESS

In the design of stressed-skin structures, consideration must often be given to the critical stresses for a sheet under a combination of shear and direct stress. The upper surface of an airplane wing in flight, for example, may be subjected to combined shear and compressive stress, while at the same time the lower surface is subjected to combined shear and tensile stress. Under this condition, the upper surface may buckle at a lower compressive stress than if the shear were not present, and the critical shear stress for the lower surface will be increased by the presence of the tensile stress. In order to gain a more complete understanding of this problem as applied to flat plates, the basic problems of compression alone and shear alone have each been studied, and the results of these studies have been used in investigating the action of plates under combined stress.

Compression alone.- A theoretical study of the critical stress for a long plate, subjected to longitudinal compression, with equal elastic restraints along the side edges, resulted in the preparation of the chart of figure 15 (see reference 4), which gives the coefficient k in the general plate-buckling formula

$$\frac{\sigma_{cr}}{\eta} = k \frac{\pi^2 E t^2}{12(1-\mu^2)b^2} \qquad (6)$$

A similar chart has been prepared for an outstanding flange and is presented in reference 5.

L-466

The parameter $4S_o b/\eta D$ in figure 15 is called the restraint coefficient,

where

S_o stiffness per unit length of elastic restraining medium, or ratio of moment per unit length at any point along the length of the medium to the rotation in quarter-radians at that point

b width of plate

D flexural stiffness of plate per unit length $\left[\frac{Et^3}{12(1-\mu^2)}\right]$

t thickness of plate

If the edge restraint is provided by other flat plates, the value of S_o is the appropriate stiffness as defined in the section on moment-distribution methods. The numerical value of S_o can therefore be obtained from the tables of reference 3.

If the edge restraint is provided by a sturdy stiffener, defined as a stiffener of such proportions that it does not suffer cross-sectional distortion when moments are applied to some part of the cross section, the value of $4S_o b/\eta D$ is (reference 8)

$$\frac{4S_o b}{\eta D} = \frac{\pi^2 b}{\lambda^2 \eta D}\left(\overline{G}J - \sigma I_p + \frac{\pi^2}{\lambda^2}\overline{E}C_{BT}\right) \qquad (7)$$

where

λ half-wave length of buckles

$\overline{G}J$ effective St. Venant torsional stiffness of stiffener

σ compressive stress in stiffener

I_p polar moment of inertia of stiffener sectional area about axis of rotation

$\overline{E}$ effective modulus of elasticity

C_{BT} torsion-bending constant of stiffener sectional area about axis of rotation at or near edge of plate

Shear alone.- A study of the critical stress for plates under shear similar to that for plates under compression has been made in reference 9. In this reference, a chart similar to figure 15 is presented for the determination of the coefficient in the formula for the critical shear stress. There is also presented in reference 9 a tentative curve that shows the variation of the effective modulus for plates in shear with the shear stress for 24S-T aluminum alloy.

Combined shear and direct stress.- A theoretical study of the critical stress for plates subjected to combined shear and compression has been made in reference 10. For an infinitely long flat plate supported and with equal elastic restraints against rotation along the edges, it was found that the combination of direct stress and shear causing instability may be determined, for practical engineering use, by the equation

$$R_c + R_s^2 = 1 \qquad (8)$$

where

R_c ratio of direct stress when buckling occurs in combined shear and direct stress to compressive stress when buckling occurs in pure compression. Tension is regarded as negative compression

R_s ratio of shear stress when buckling occurs in combined shear and direct stress to shear stress when buckling occurs in pure shear

This conclusion is illustrated in figures 16 and 17. In these figures, the plotted points represent the exact values of critical stress computed from the theoretical solution. The various symbols represent different constant values of the restraint coefficient ϵ between 0 and ∞, which cover the entire range from simple support to fixed edges, and one case in which ϵ varies with the wave length λ.

CRITICAL COMPRESSIVE STRESS FOR CURVED SHEET

Because the skin between stiffeners on the surface of airplanes is curved to the contour of the wing or fuselage, it is important to investigate the extent to which this curvature influences the critical stress.

In the course of an experimental study (reference 11) of the effect of curvature on the critical compressive stress for plate elements between longitudinal stiffeners, a number of specimens of the type shown in figure 18 were tested. The stiffeners at the edges of the sheet were so proportioned as to force buckling to occur in the sheet at a load lower than the lowest critical load for instability of the stiffeners and to provide adequate support against deflection normal to the sheet, without having excessive area in the stiffeners.

In figure 19 are presented the results of tests on the group of specimens with the dimensions shown in figure 18 and with various radii of curvature r. For the three specimens with r/t less than 500, the critical stress for the points represented by circles in figure 19 was the observed stress at which buckles occurred suddenly with a snap-diaphragm action accompanied by a loud report. For all specimens with r/t greater than 500, the critical stress represented by the circles was determined from an analysis of the growth of buckles by the Southwell method as generalized in reference 12. The crosses in figure 19 represent the critical stresses as determined by the methods described in the section on COMPRESSION TESTS OF CHANNEL, Z-, AND H-SECTIONS.

The curves A, B, and C in figure 19 are the curves given in figures 7 and 9 of reference 13, which represent the NACA study of circular cylinders in compression. Curves A and B, respectively, are the graphs of the equations

$$\frac{\sigma_{cr}}{E} = 0.605\,\frac{t}{r} \quad \text{and} \quad \frac{\sigma_{cr}}{E} = 0.363\,\frac{t}{r}$$

The plotted points in figures 7 and 9 of reference 13, representing the compressive strength of carefully constructed cylinders, scattered between curves B and C.

The dashed curve in figure 19 is a graph of the equation

$$\frac{\sigma_{cr}}{E} = 0.6 \left[\frac{k'\pi^2}{12(1-\mu^2)} \left(\frac{t}{b}\right)^2 + \frac{1}{k'\pi^2} \left(\frac{b}{r}\right)^2 \right] \qquad (9)$$

where

$k' = \frac{k}{0.6}$

k coefficient for critical stress of sheet when flat

b width of sheet between stiffeners

t thickness of sheet

r radius of curvature

This equation is a modification of the theoretical equation derived in reference 14, which is a generalization of equation (276) of reference 15 to include all degrees of edge restraint instead of simple support alone. The value of k was chosen to make the curve agree with the experimental points plotted as circles for $r/t = \infty$.

Regardless of whether the Southwell method or the method given in reference 7 is used to establish experimental critical stresses, it appears from the data that the effect of curvature cannot be relied upon to follow consistently the gradual increase in critical stress with increase in curvature represented by equation (9). The data of figure 19, together with similar data also presented in reference 11, lead to the conclusion that for practical engineering use the critical compressive stress for a curved sheet between stiffeners is equal to the larger of the following values:

(a) The critical compressive stress for an unstiffened circular cylinder of the same radius-thickness ratio

(b) The critical compressive stress for the same sheet when flat

EFFECT OF AN OUTWARD-ACTING NORMAL PRESSURE ON THE CRITICAL STRESS OF CURVED SHEET

No consideration has thus far been given to the effect of normal pressure on the critical stress. The beneficial effect of the suction pressures on the upper surface of wings, however, should be considered. This problem is being studied by the NACA and two papers (references 16 and 17) have been prepared to present the results of preliminary experimental work.

Examples of the extent to which an outward-acting normal pressure raises the critical stress for curved sheet are shown in figures 20 and 21 for the specimen of figure 22. The numbers beside the experimental points in figures 20 and 21 give the order in which the various tests were made. For both compression and shear, an outward-acting normal pressure raised the critical stress, which varied approximately linearly with the pressure.

CONCLUDING REMARKS

This paper is a review of a part of the work done by the NACA on the subject of the critical stresses for plates in compression and in shear, as well as in combined direct stress and shear. Although some theoretical methods are presented, the main emphasis is on the practical significance and use of the results of both theoretical studies and laboratory tests concerned with the buckling of plates.

Langley Memorial Aeronautical Laboratory,
National Advisory Committee for Aeronautics,
Langley Field, Va.

REFERENCES

1. Lundquist, Eugene E.: Stability of Structural Members under Axial Load. NACA TN No. 617, 1937.

2. Lundquist, Eugene E., Stowell, Elbridge Z., and Schuette, Evan H.: Principles of Moment Distribution Applied to Stability of Structures Composed of Bars or Plates. NACA ARR No. 3K06, 1943.

3. Kroll, W. D.: Tables of Stiffness and Carry-Over Factor for Flat Rectangular Plates under Compression. NACA ARR No. 3K27, 1943.

4. Lundquist, Eugene E., and Stowell, Elbridge Z.: Critical Compressive Stress for Flat Rectangular Plates Supported along All Edges and Elastically Restrained against Rotation along the Unloaded Edges. NACA Rep. No. 733, 1942.

5. Lundquist, Eugene E., and Stowell, Elbridge Z.: Critical Compressive Stress for Outstanding Flanges. NACA Rep. No. 734, 1942.

6. Kroll, W. D., Fisher, Gordon P., and Heimerl, George J.: Charts for Calculation of the Critical Stress for Local Instability of Columns with I-, Z-, Channel, and Rectangular-Tube Section. NACA ARR No. 3K04, 1943.

7. Heimerl, George J., and Roy, J. Albert: Preliminary Report on Tests of 24S-T Aluminum-Alloy Columns of Z-, Channel, and H-Section That Develop Local Instability. NACA RB No. 3J27, 1943.

8. Lundquist, Eugene E., and Stowell, Elbridge Z.: Restraint Provided a Flat Rectangular Plate by a Sturdy Stiffener along an Edge of the Plate. NACA Rep. No. 735, 1942.

9. Stowell, Elbridge Z.: Critical Shear Stress of an Infinitely Long Flat Plate with Equal Elastic Restraints against Rotation along the Parallel Edges. NACA ARR No. 3K12, 1943.

10. Stowell, Elbridge Z., and Schwartz, Edward B.: Critical Stress for an Infinitely Long Flat Plate with Elastically Restrained Edges under Combined Shear and Direct Stress. NACA ARR No. 3K13, 1943.

11. Crate, Harold, and Levin, L. Ross: Data on Buckling Strength of Curved Sheet in Compression. NACA ARR No. 3J04, 1943.

12. Lundquist, Eugene E.: Generalized Analysis of Experimental Observations in Problems of Elastic Stability. NACA TN No. 658, 1938.

13. Lundquist, Eugene E.: Strength Tests of Thin-Walled Duralumin Cylinders in Compression. NACA Rep. No. 473, 1933.

14. Stowell, Elbridge Z.: Critical Compressive Stress for Curved Sheet Supported along all Edges and Elastically Restrained against Rotation along the Unloaded Edges. NACA RB No. 3I07, 1943.

15. Timoshenko, S.: Theory of Elastic Stability. McGraw-Hill Book Co., Inc., New York, N. Y., 1936.

16. Rafel, Norman: Effect of Normal Pressure on the Critical Compressive Stress of Curved Sheet. NACA RB, Nov. 1942.

17. Rafel, Norman: Effect of Normal Pressure on the Critical Shear Stress of Curved Sheet. NACA RB, Jan. 1943.

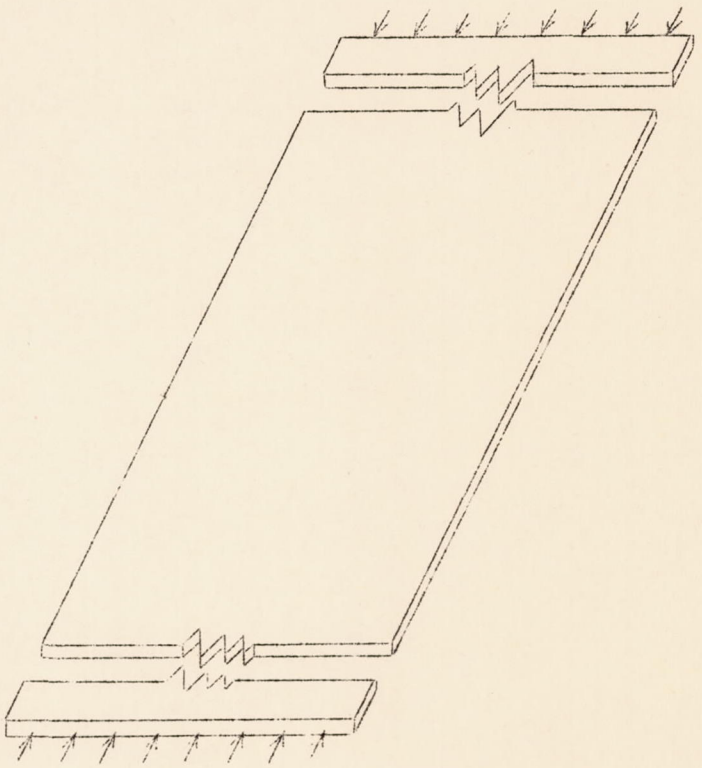

Figure 1.—Infinitely long flat plate under compressive load. (From reference 2.)

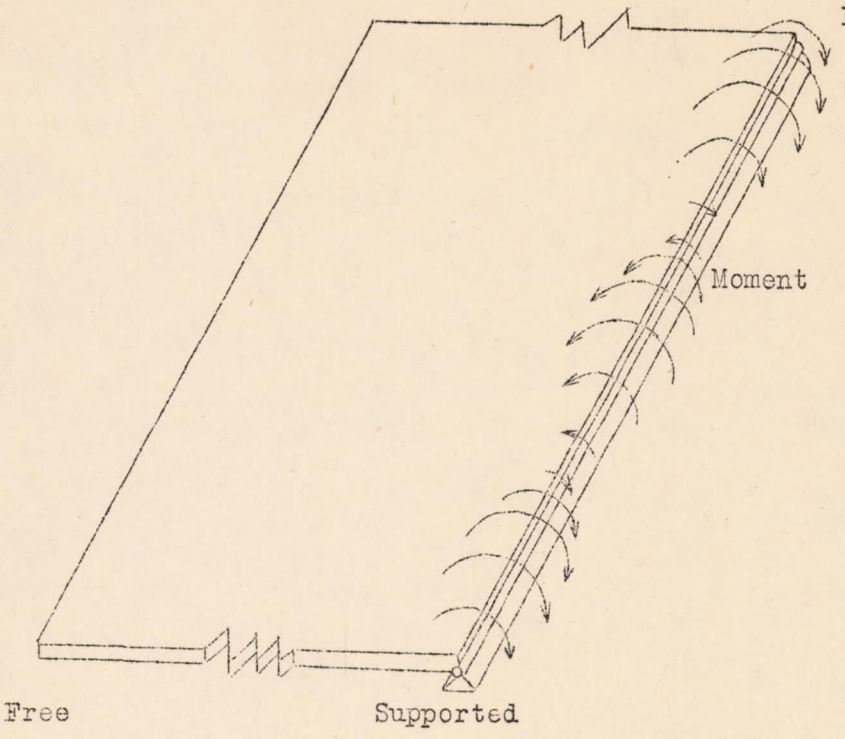

Figure 2.- Plate with moment applied at near edge, far edge free. (From reference 2.)

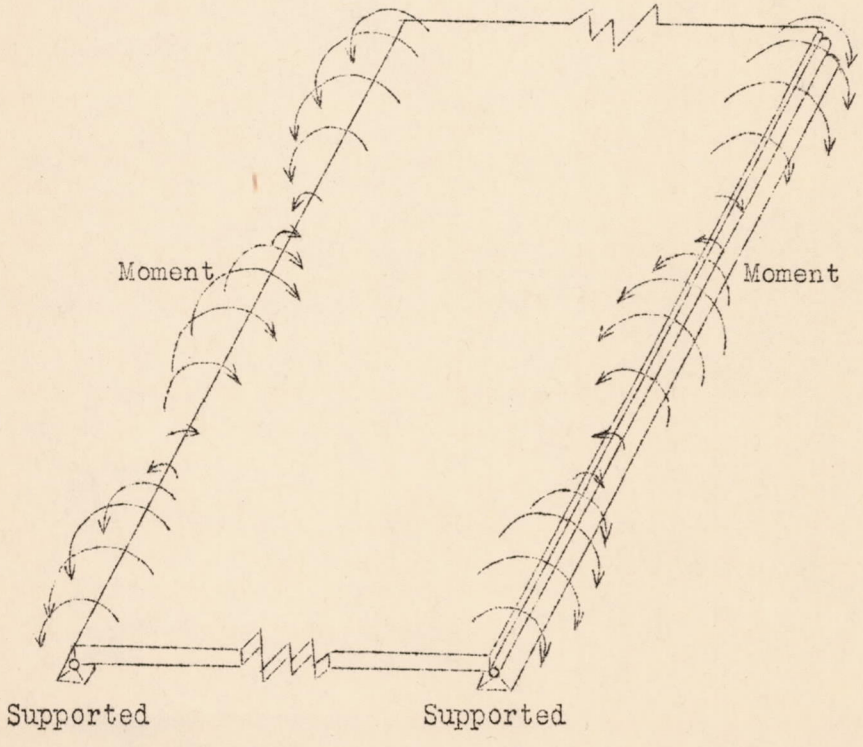

Figure 3.- Plate with moment applied at near edge, equal and opposite moment at far edge. (From reference 2.)

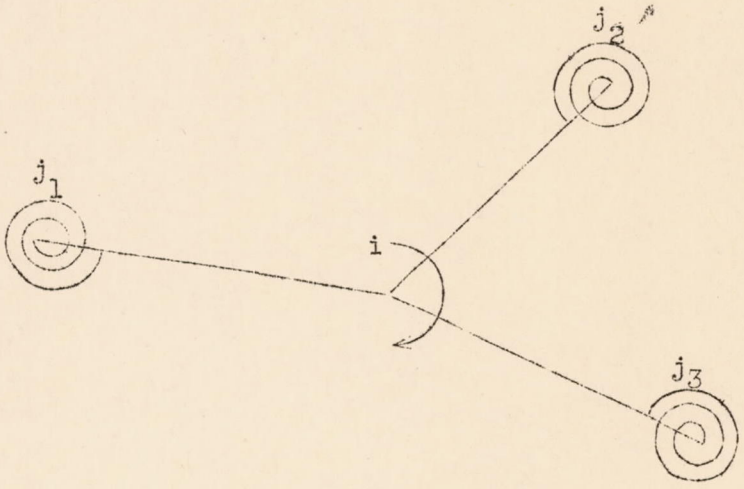

Figure 4.- End view of assembly of plates with a common edge i. (From reference 2.)

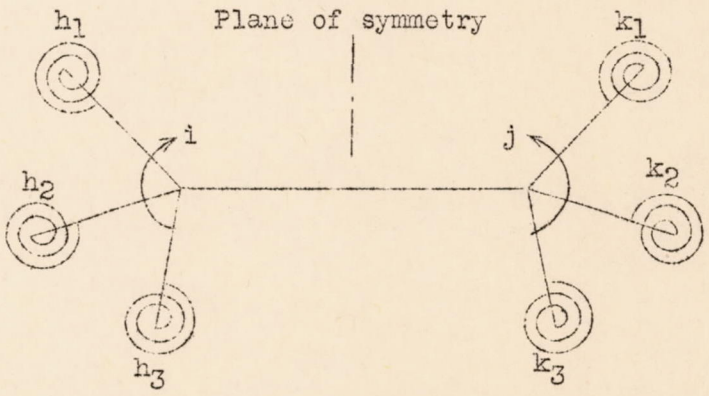

Figure 5.- End view of assembly of plates symmetrical about plate ij. (From reference 2.)

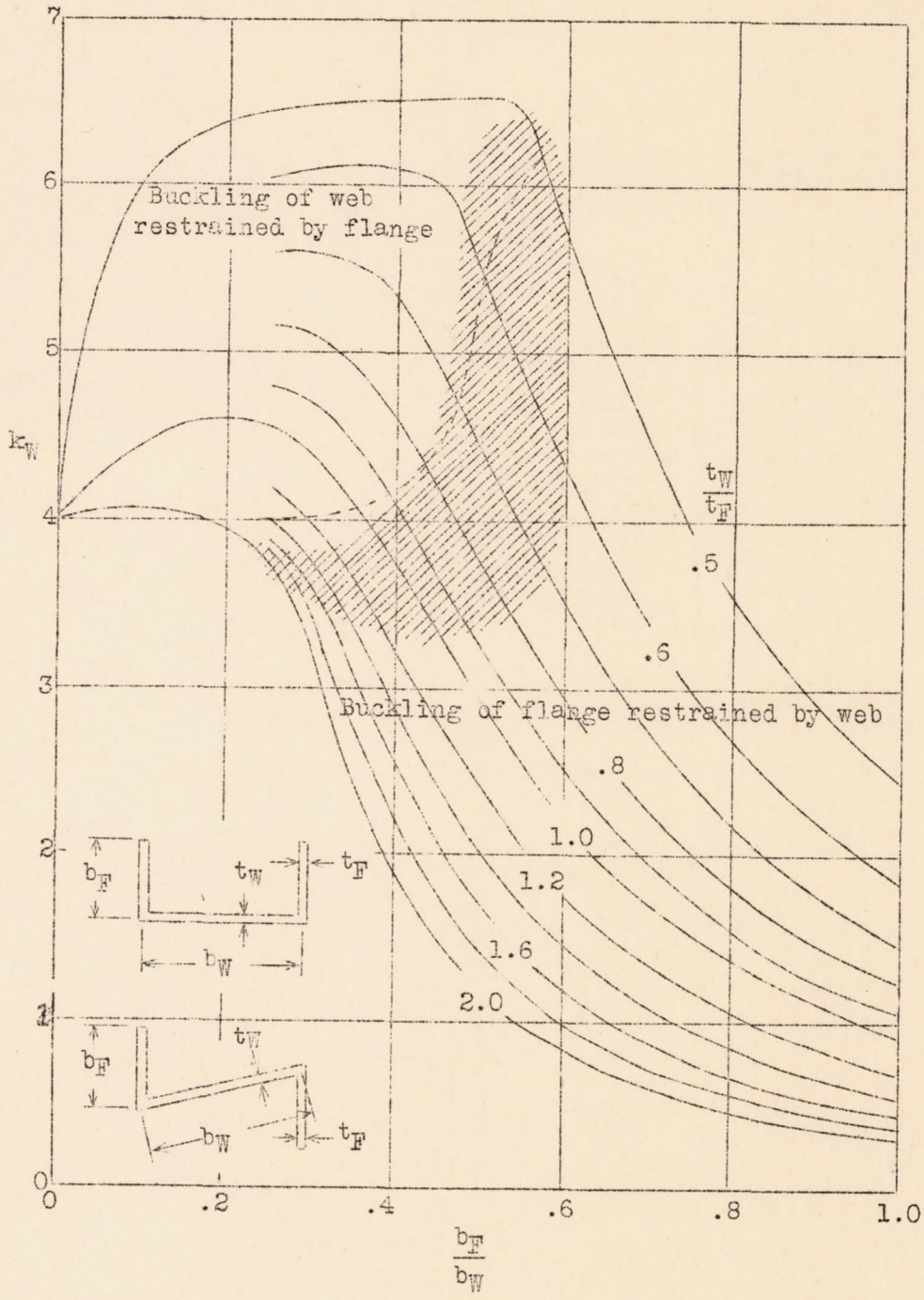

Figure 6.- Minimum values of k_w for centrally loaded columns of channel and Z-section. (Adapted from reference 6.)

$$\frac{\sigma_{cr}}{\eta} = \frac{k_w \pi^2 E t_w^2}{12(1-\mu^2) b_w^2}$$

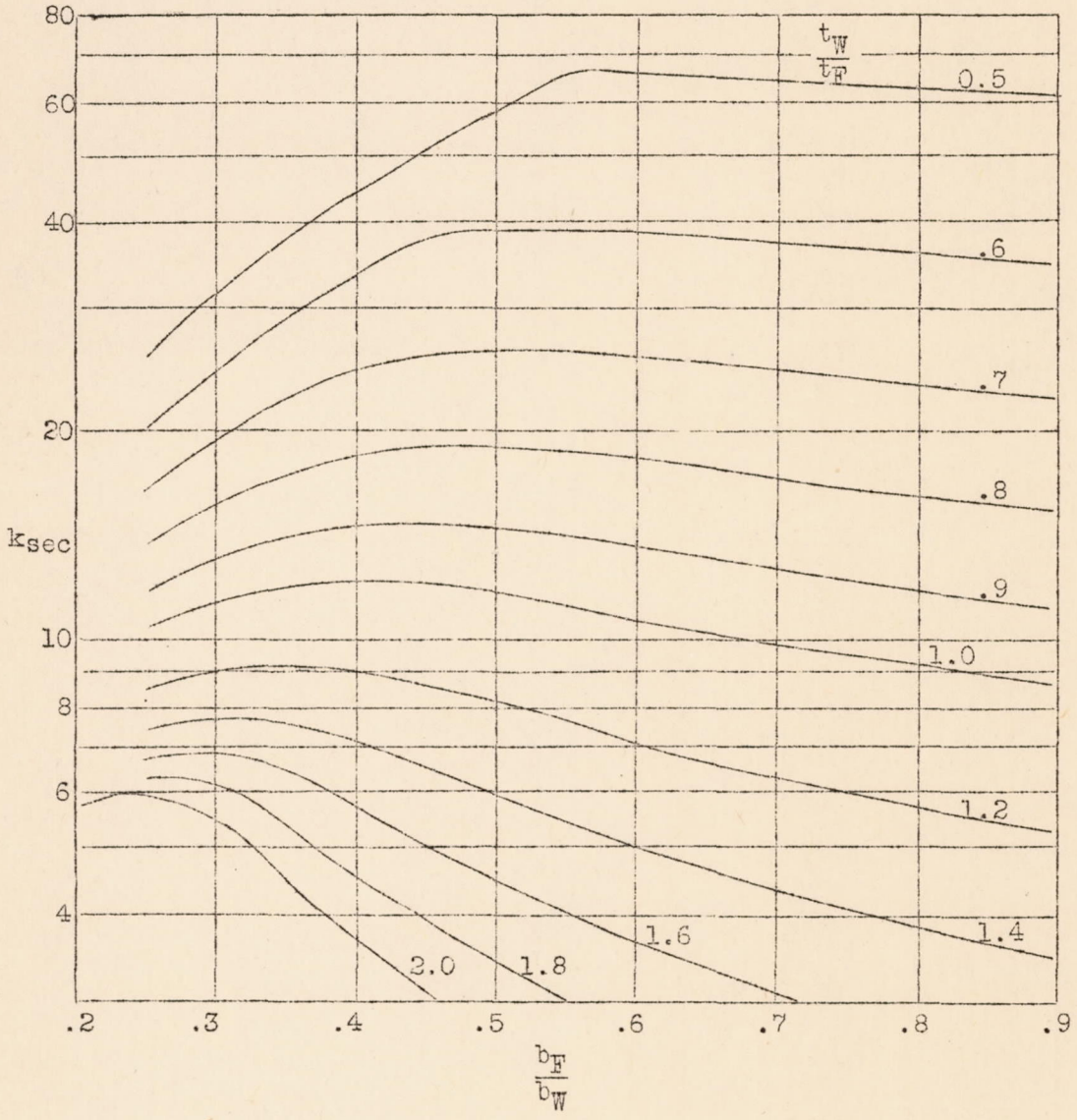

Figure 7.- Values of k_{sec} for centrally loaded columns of channel and Z-section. (Adapted from reference 6.)

$$\frac{\sigma_{cr}}{\eta} = \frac{k_{sec}\pi^2 E}{12(1-\mu^2)}\left(\frac{t_W}{A}\right)^2$$

L-466

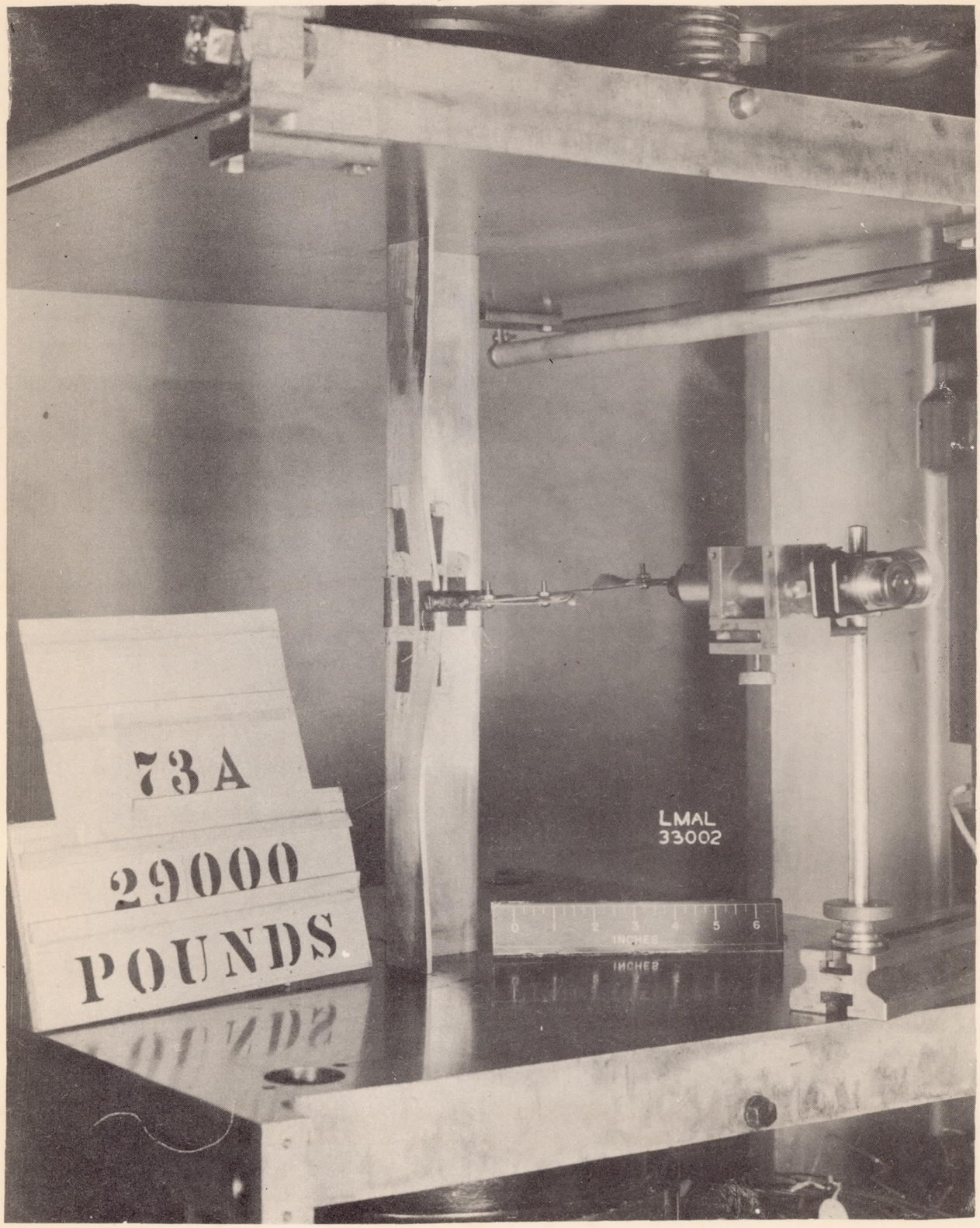

Figure 8.- Column of z-section after buckling. (From reference 7.)

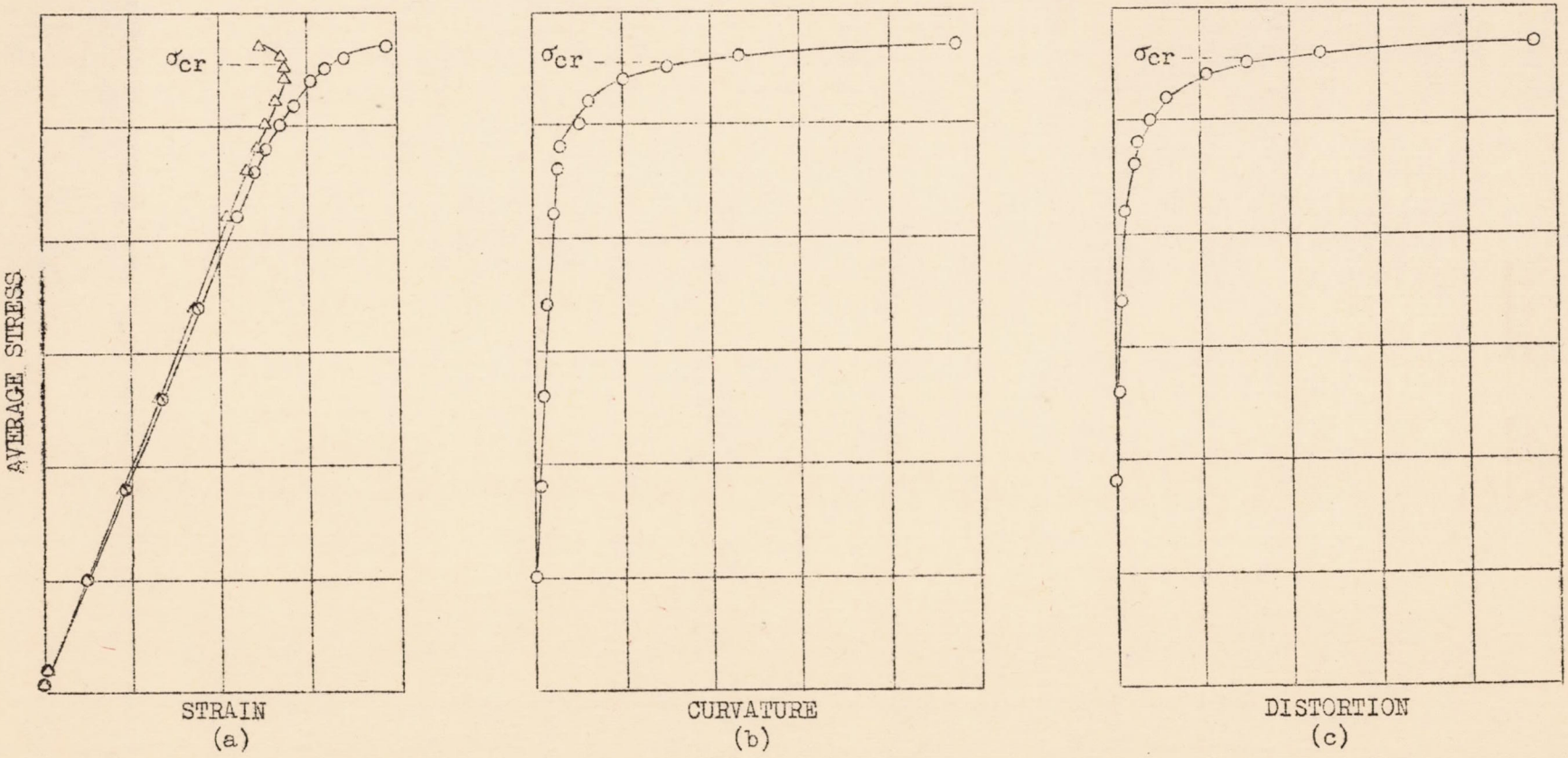

Figure 9.- Typical test data for columns of channel, Z-, or H-section. (Adapted from reference 7.)

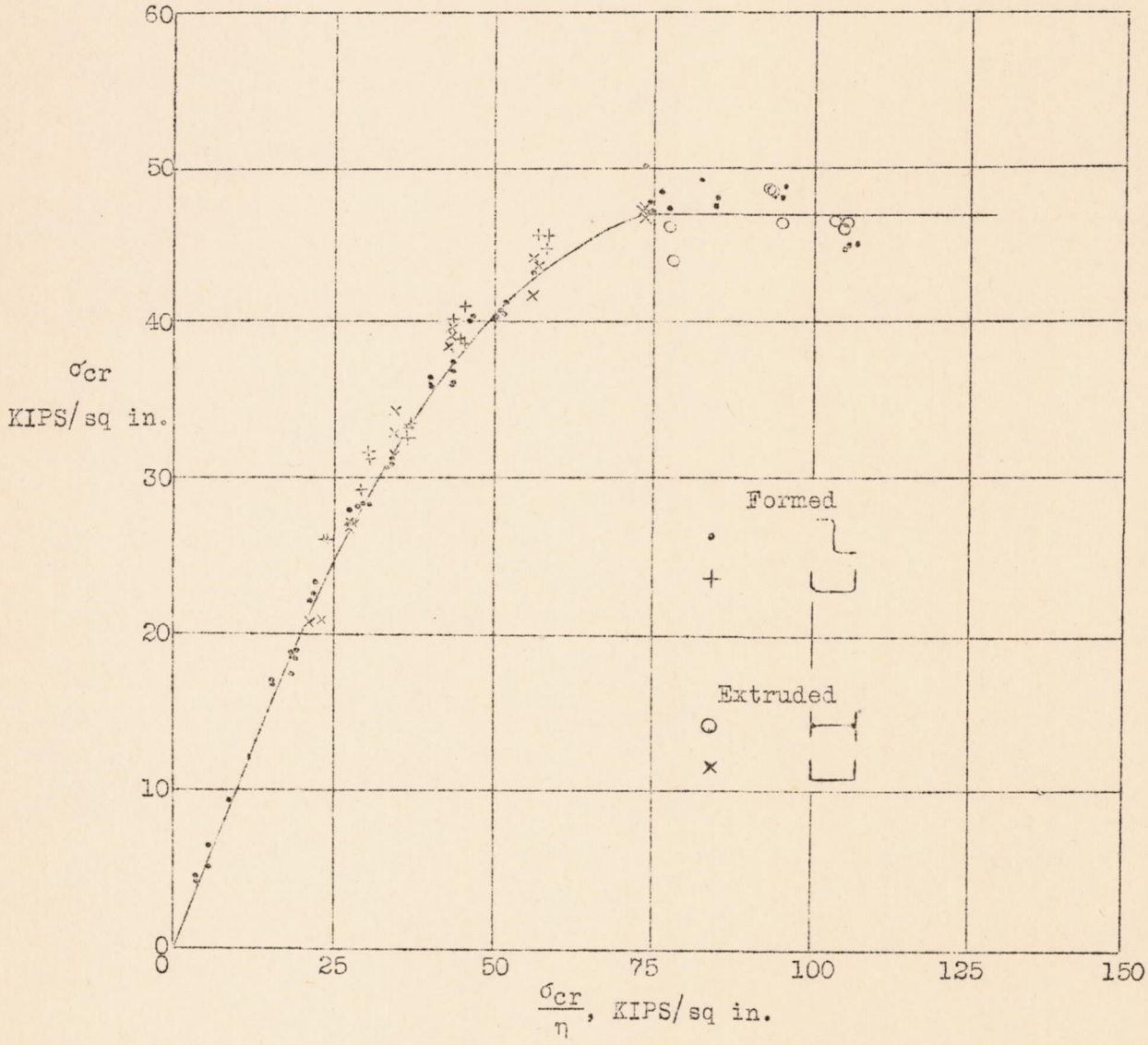

Figure 10.- Variation of σ_{cr} with σ_{cr}/η for 24S-T aluminum-alloy columns of channel, Z-, or H-section that fail by instability of web or flanges. (Adapted from reference 7.)

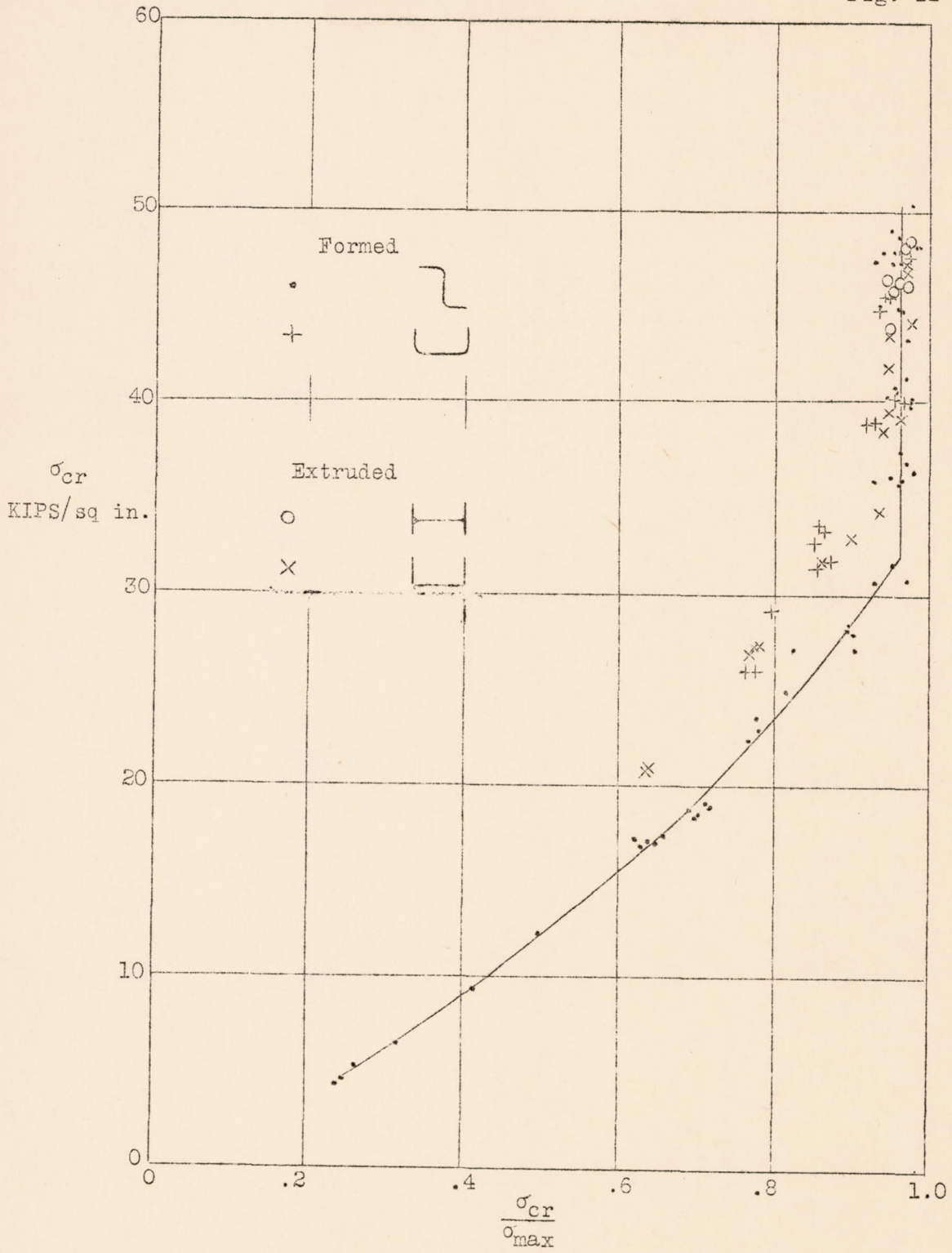

Figure 11.- Variation of σ_{cr} with σ_{cr}/σ_{max} for 24S-T aluminum-alloy columns of channel, Z-, or H-section that fail by instability of web or flanges. (Adapted from reference 7.)

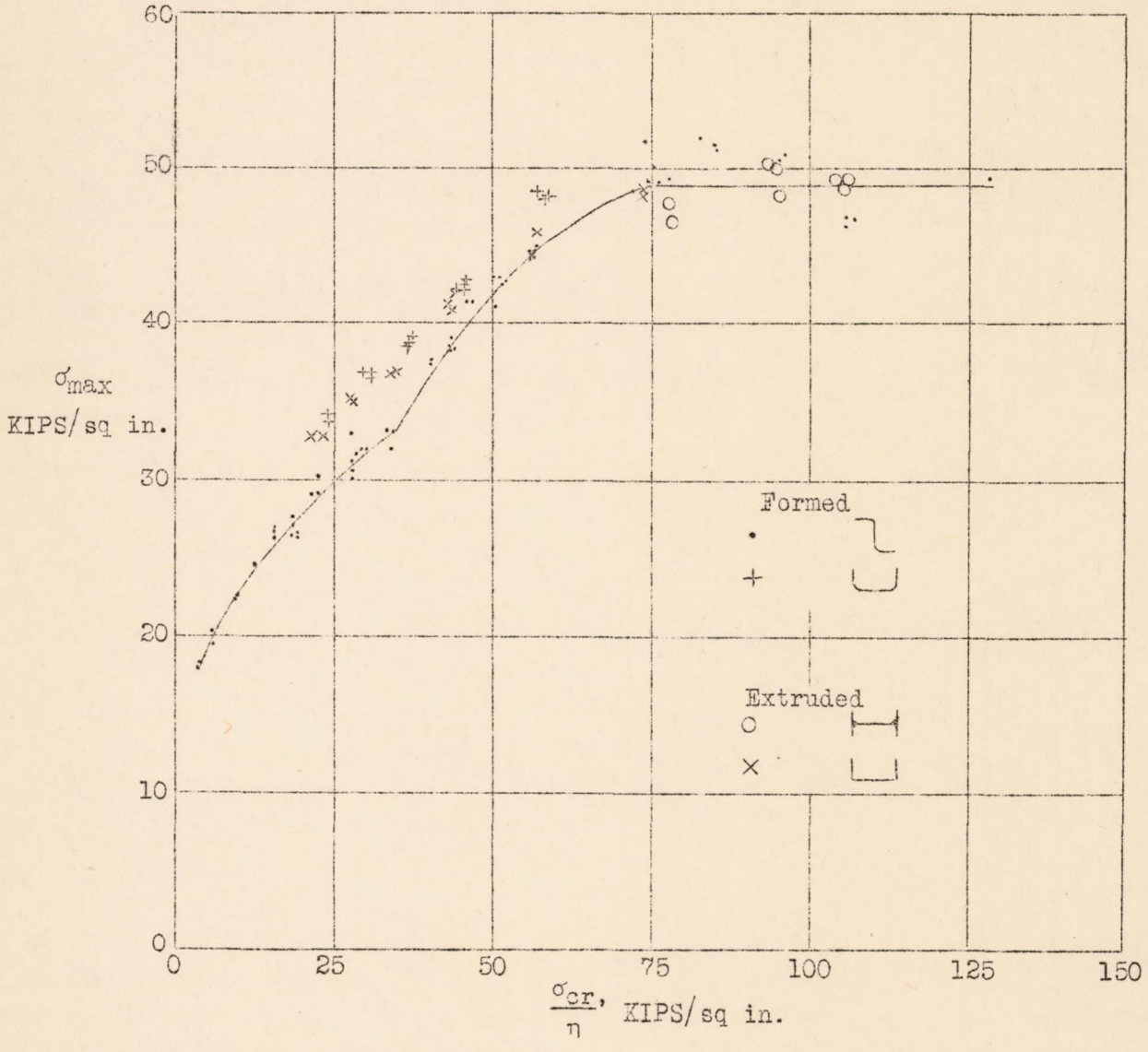

Figure 12.- Variation of σ_{max} with σ_{cr}/η for 24S-T aluminum-alloy columns of channel, Z-, or H-section that fail by instability of web or flanges. (Adapted from reference 7.)

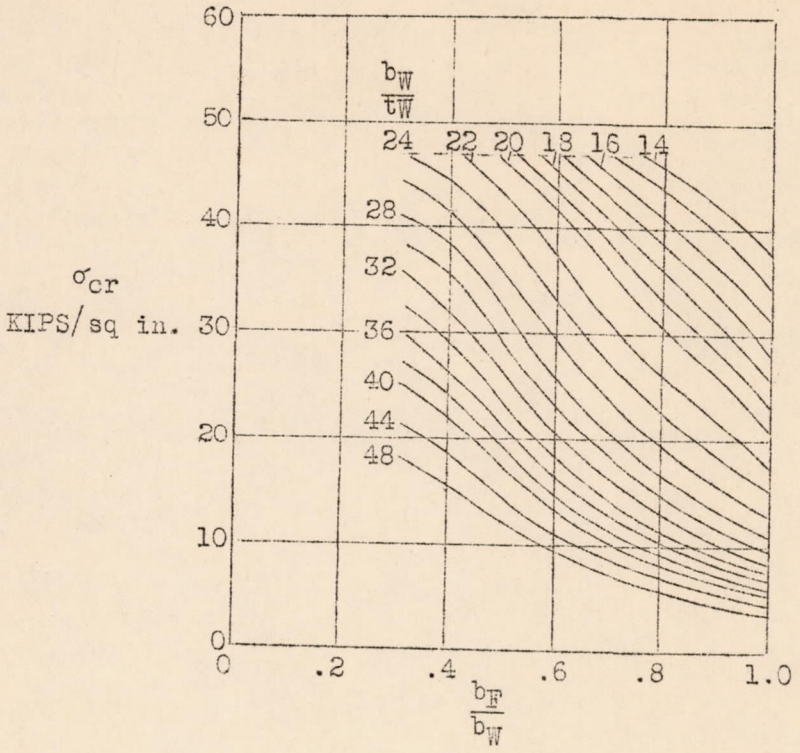

Figure 13.- Design chart for critical stress of 24S-T aluminum-alloy columns of Z-section that fail by instability of web or flanges. (From reference 7.)

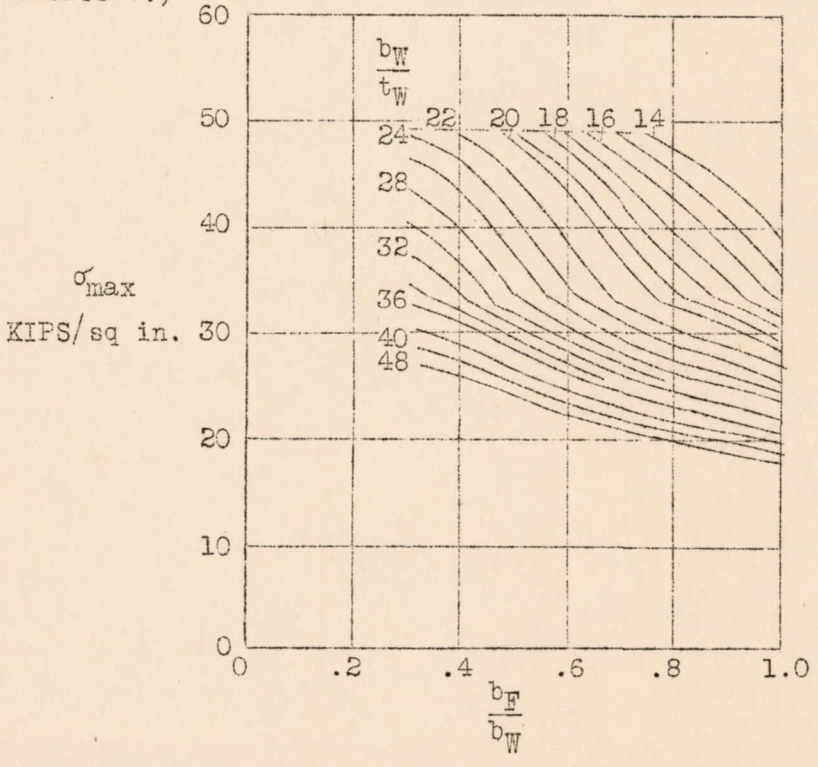

Figure 14.- Design chart for maximum stress of 24S-T aluminum-alloy columns of Z-section that fail by instability of web or flanges. (From reference 7.)

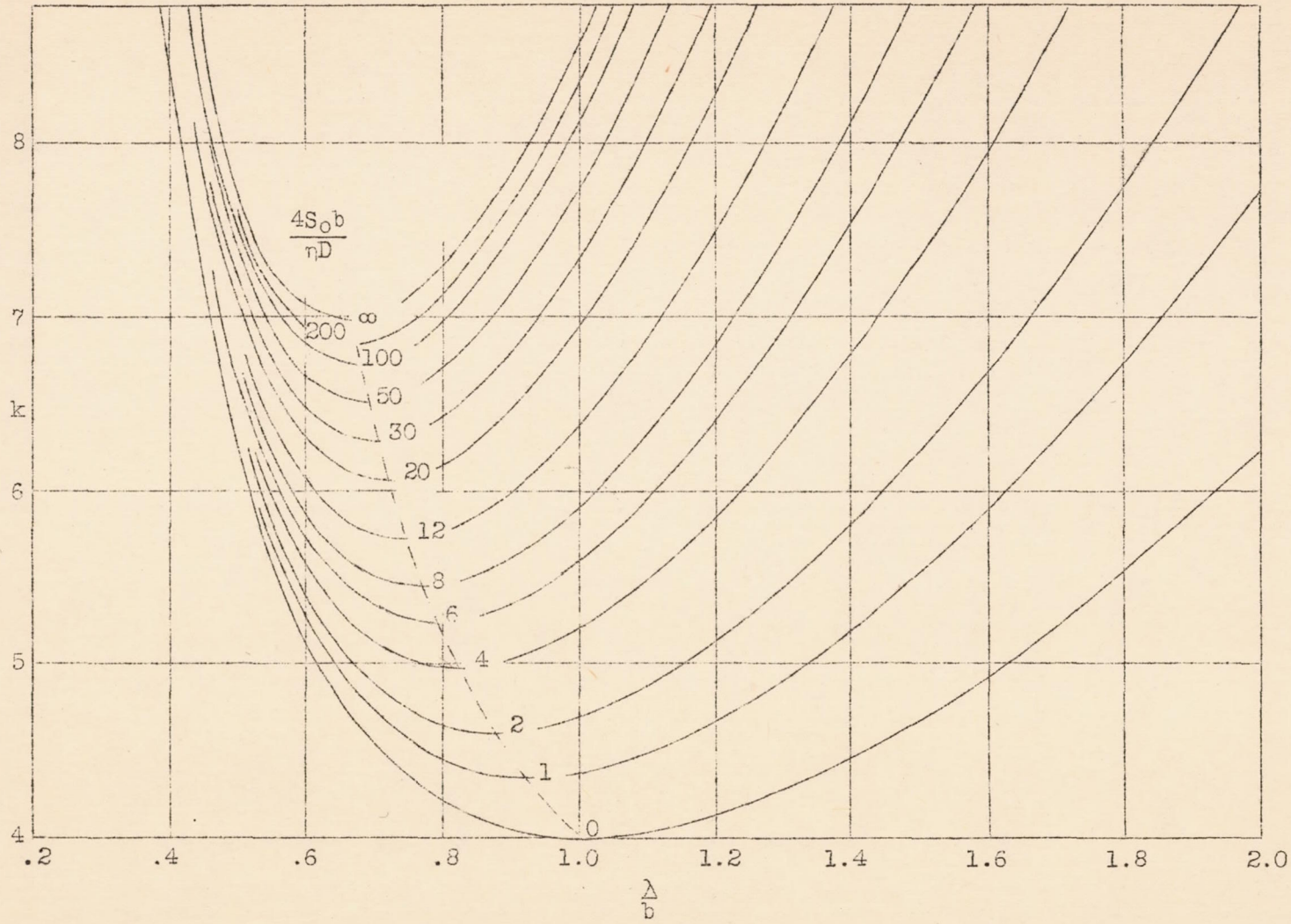

Figure 15.- Design chart for flat plates giving values of k for equal restraint coefficients $4S_0b/\eta D$ on each side edge of the plate. (Adapted from reference 4.)

$$\frac{\sigma_{cr}}{\eta} = \frac{k\pi^2 E t^2}{12(1-\mu^2)b^2}$$

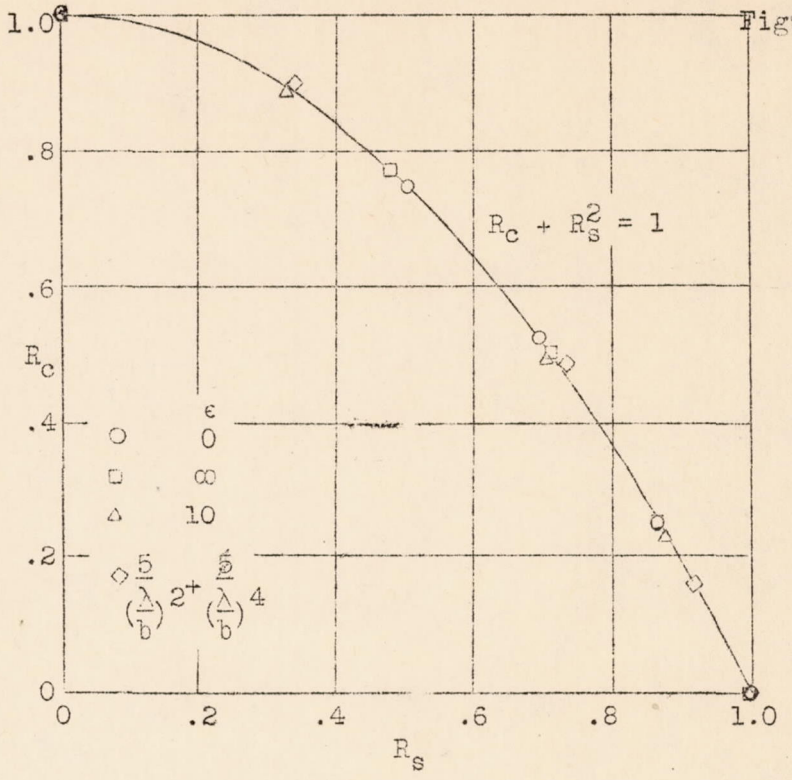

Figure 16.- Interaction curve for critical stress of a flat plate under combined shear and compression. (Adapted from reference 10.)

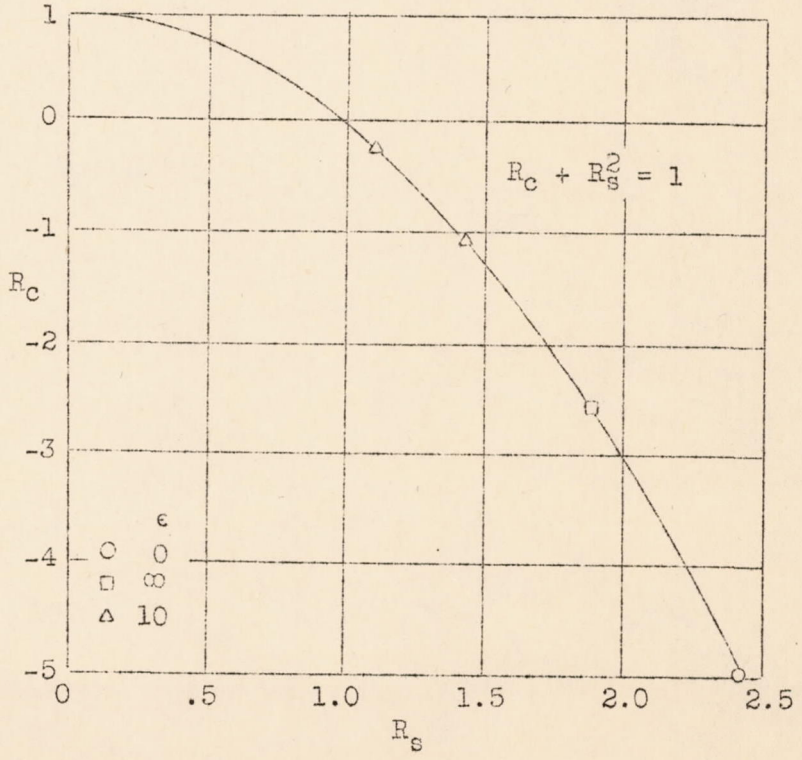

Figure 17.- Interaction curve for critical stress of a flat plate under combined shear and compression or tension. (Adapted from reference 10.)

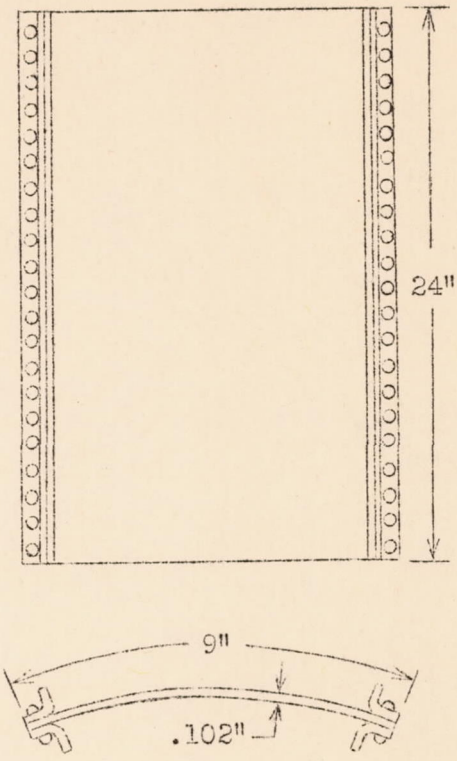

Figure 18.- Dimensions of curved-sheet specimen. (From reference 11.)

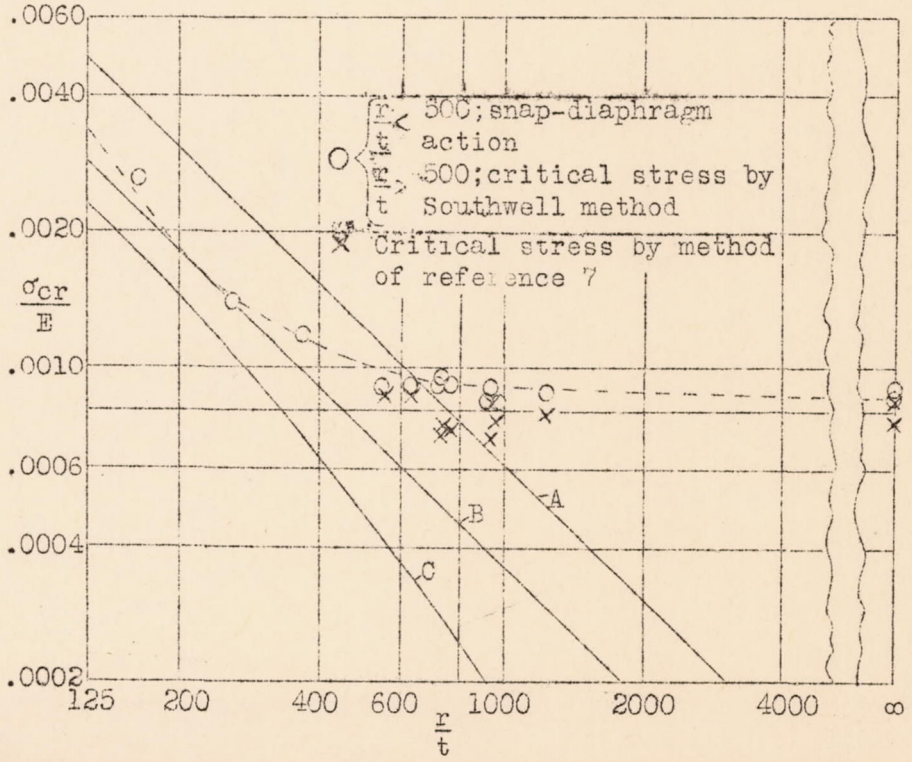

Figure 19.- Critical compressive stress for 24S-T aluminum-alloy curved sheet between stiffeners for specimens of type shown in figure 18. (Adapted from reference 11.)

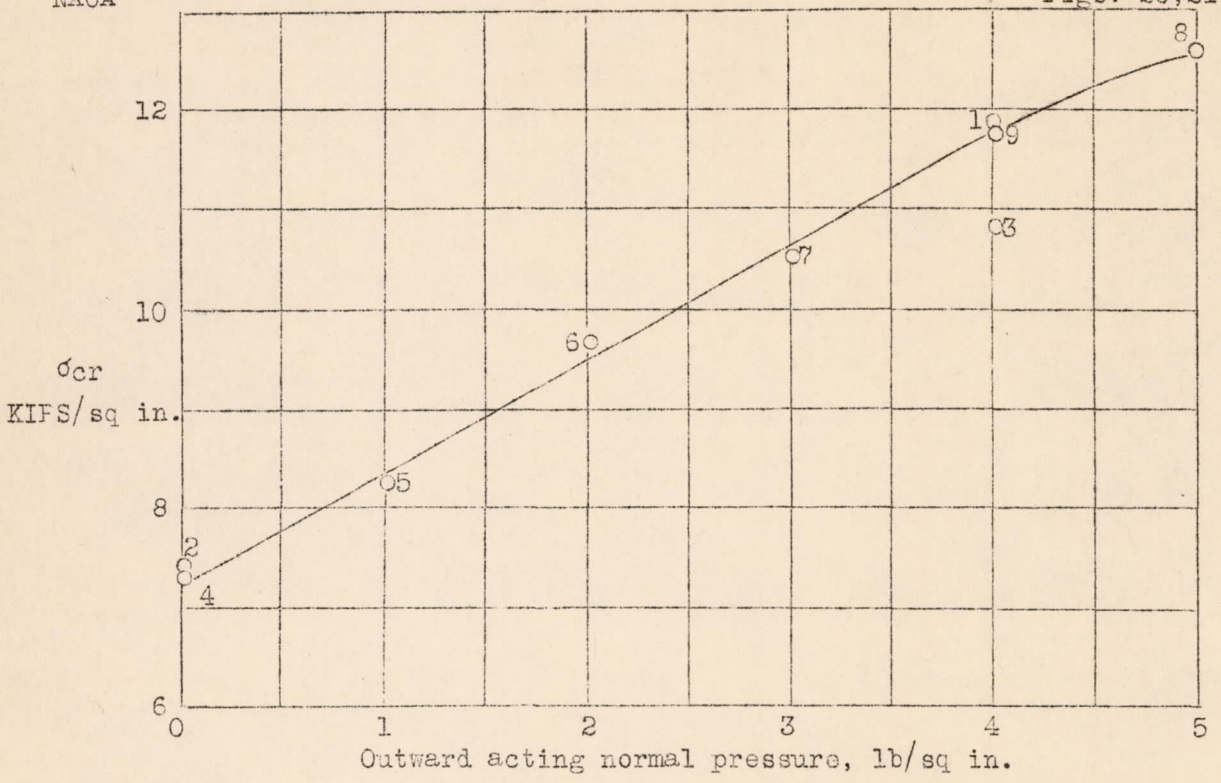

Figure 20.- Effect of normal pressure on critical compressive stress of curved sheet for specimen of figure 22. (Adapted from reference 16.)

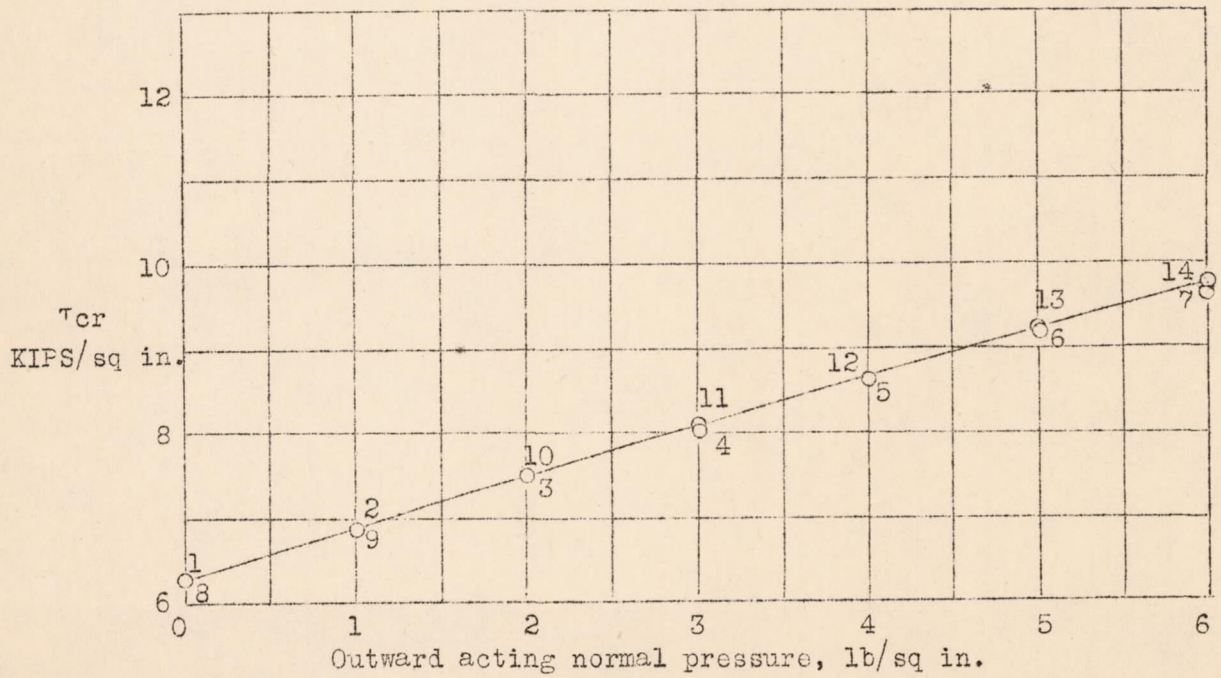

Figure 21.- Effect of normal pressure on critical shear stress of curved sheet for specimen of figure 22. (Adapted from reference 17.)

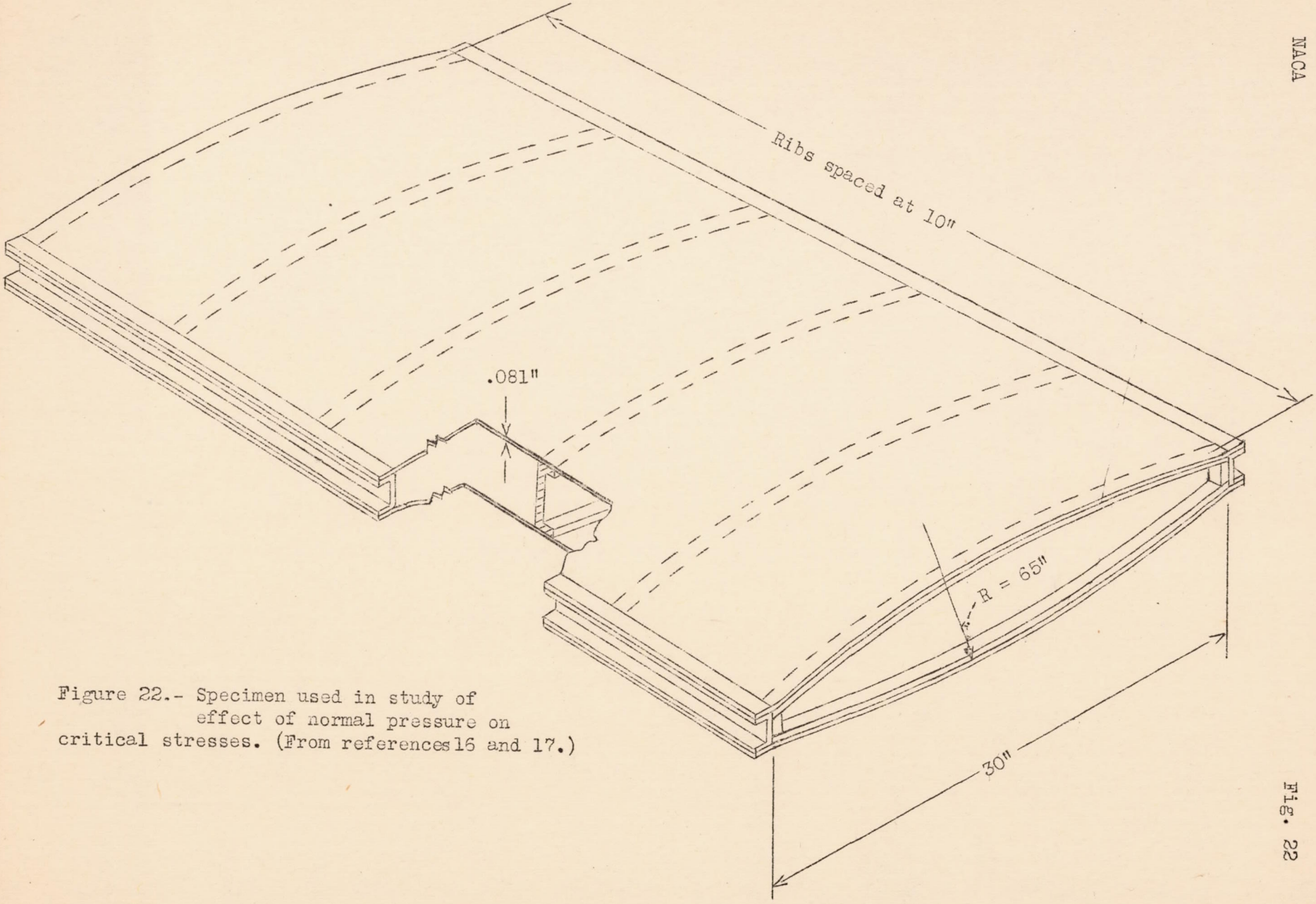

Figure 22.- Specimen used in study of effect of normal pressure on critical stresses. (From references 16 and 17.)